ELSEVIER

Journal of Power Sources 96 (2001) 376–384

JOURNAL OF POWER SOURCES

www.elsevier.com/locate/jpowsour

Synthesis and characterization of lithium aluminum-doped spinel ($LiAl_xMn_{2-x}O_4$) for lithium secondary battery

Yun-Sung Lee, Naoki Kumada, Masaki Yoshio*

Department of Applied Chemistry, Saga University, 1 Honjo, Saga 840-8502, Japan

Received 7 October 1999; received in revised form 6 November 2000; accepted 8 November 2000

Abstract

$LiAl_xMn_{2-x}O_4$ has been synthesized using various aluminum starting materials, such as $Al(NO_3)_3$, $Al(OH)_3$, AlF_3 and Al_2O_3 at 600–800°C for 20 h in air or oxygen atmosphere. A melt-impregnation method was used to synthesize Al-doped spinel with good battery performance in this research. The Al-doped content and the intensity ratio of (3 1 1)/(4 0 0) peaks can be important parameters in synthesizing Al-doped spinel which satisfies the requirements of high discharge capacity and good cycleability at the same time. The decrease in Mn^{3+} ion by Al substitution induces a high average oxidation state of Mn ion in the $LiAl_xMn_{2-x}O_4$ material. The electrochemical behavior of all samples was studied in Li/$LiPF_6$-EC/DMC (1:2 by volume)/$LiAl_xMn_{2-x}O_4$ cells. Especially, the initial and last discharge capacity of $LiAl_{0.09}Mn_{1.97}O_4$ using LiOH, Mn_3O_4 and $Al(OH)_3$ complex were 128.7 and 115.5 mAh/g after 100 cycles. The Al substitution in $LiMn_2O_4$ was an excellent method of enhancing the cycleability of stoichiometric spinel during electrochemical cycling.

Keywords: Spinel; Al-doped spinel; Cycleability; The intensity ratio of (3 1 1)/(4 0 0) peaks; Lithium battery

1. Introduction

The commercial lithium battery with high energy density and good cycle life has been studied as a power source for portable electronics. Many researchers [1–4] have investigated various cathode materials for the lithium secondary battery such as a layered oxide; $LiMO_2$ (M = Co, Ni, etc.).

$LiCoO_2$ involves many problems such as high cost, environmental aspects and low practical capacity. Although, $LiNiO_2$ has a larger practical capacity than $LiCoO_2$, it is highly possible for exothermic decomposition of the oxide to occur, releasing oxygen at high temperature. This was reported as the main difficulty in developing pure $LiNiO_2$ cathode material for emission-free vehicles [5,6].

$LiMn_2O_4$ has been widely investigated because of its cost performance, environmental merit, easy preparation and stabilization at high temperature compared with other cathode materials [7–10].

However, $LiMn_2O_4$ showed significant capacity fading and poor cycleability, when it was cycled in the (3 + 4) voltage range. In the 3 V region, Jahn–Teller distortion was introduced into the spinel structure, reducing the crystal symmetry (cubic → tetragonal, *c*/*a* ratio of unit cell increased 16%), this was the worst problem that led to capacity fading in this range. In the 4 V region, it showed excellent cycleability at room temperature. However, it showed many indications of poor cycleability in the high temperature region. The reasons for capacity loss are the electrochemical reaction of the electrolyte solution at high voltage and slow dissolution of the spinel $LiMn_2O_4$ electrode into the electrolyte according to the disproportional reaction: $2Mn^{3+} \rightarrow Mn^{4+} + Mn^{2+}$.

Oh et al. [11,12] announced that spinel dissolution is introduced by acids which are generated as a result of electrochemical oxidation of solvent molecules on the cathodes and the polarization loss due to cell resistance increase.

In our previous paper [13], we had already reported that one reason for capacity fading was the change in the two-phase structure of spinel $LiMn_2O_4$ in the high voltage region. Although, it can remain a two-phase structure in the low voltage region, it was transformed into a one-phase structure, which was a more stable state than the two-phase structure, when it was cycled at high temperature.

Many researchers tried to solve the above problems and synthesized lithium rich spinels and metal ion-doped spinels such as $LiM_xMn_{2-x}O_4$ (M = Co, Ni, Al, Mg, Ga, etc.). In

* Corresponding author. Tel.: +81-952-28-8673; fax: +81-952-28-8591.
E-mail address: yoshio@ccs.ce.saga-u.ac.jp (M. Yoshio).

0378-7753/01/$ – see front matter
PII: S0378-7753(00)00652-2

view of the fact, Dahn et al. [14] announced the results of doped materials for spinel and nickelate under a variety of synthesis conditions. They insisted that all researchers who want to make pure materials must be careful of the synthesis conditions, such as cooling rate and voltage region.

Recently, Strobel et al. [15] tried to synthesize $LiAlMnO_4$ and $LiMg_{0.5}Mn_{1.5}O$ materials to recover the Jahn–Teller distortion in the Li–Mn–O system. In the case of aluminum, it is easy to form a solid solution with spinel, because the ionic radius of Al^{3+} (0.57 Å) is similar to that of Mn^{3+} (0.66 Å). If one successfully substitutes Al^{3+} ion for Mn^{3+} ion, which is related to the Jahn–Teller distortion, it is possible to encourage cycleability of the spinel. In spite of these advantages, they seemed to not succeed in its substitution using aluminum acetate in their research.

We have synthesized Al-doped spinel ($LiAl_xMn_{2-x}O_4$, $x = 0.3$–0.12) with a high initial capacity and good cycleability simultaneously using a melt-impregnation method which is used to synthesize spinel in our laboratory. This method has good features for developing a long-life battery system and it can contribute of preparing Al-based powders as cathode materials for lithium secondary batteries.

In this paper, we report the results of synthesis and the electrochemical behavior of Al-doped spinel which was prepared using various aluminum starting materials.

2. Experimental

2.1. Starting materials and synthetic procedure

All $LiAl_xMn_{2-x}O_4$ samples here were prepared by the melt-impregnation method [16]. A stoichiometric amount of $LiOH{\cdot}H_2O$ (Osaka Kisida Chemical), manganese ((Mn_3O_4 and γ-MnOOH, Tosoh Chemical, Japan)) and aluminum-based materials ($Al(NO_3)_3{\cdot}9H_2O$ (Katayama Chemical, Japan), $Al(OH)_3$, AlF_3 (Wako Chemical industries, Ltd.), and nano particle size Al_2O_3 (20 wt.%, aqueous solution)) were mixed in various cationic ratios ($x = 0.3$–0.12). The starting materials and preparation conditions are summarized in Table 1. These compounds were precalcined at 300 or 450°C for 10 h in air or oxygen after grinding well in a mortar. These materials were reground and calcined at 600–900°C for 24 h in air or oxygen atmosphere to obtain the pure Al-doped spinel.

2.2. Instrumentation and cell assembly

The thermal decomposition behavior of the Al-doped precursors was examined by means of thermogravimetric analysis and differential thermal analysis using a TG-8110 thermal analyzer system (TGA, DTA, TAS 100, Rigaku Ltd., Japan). A thin Pt plate was used as the sample holder. The powder was heated at 5°C/min and cooled at 10°C/min in N_2 flow. The powder X-ray diffraction (XRD, Rint 1000, and Rigaku Ltd., Japan) using Cu Kα radiation was performed to identify the crystalline phase of materials that were prepared at different temperatures and Al contents. The measurement range was 10–80° and the step size was 0.02°. Rietveld refinement analysis was performed with XRD data to obtain the lattice parameters. In order to calculate the average oxidation state of Mn, titration with excess $FeSO_4$ solution with standard $KMnO_4$ solution was carried out. The total Mn ion was determined by a complexometric titration method, in which excess EDTA was analyzed by back titration using standard zinc solution. The sample was first dissolved in hydroxylammonium chloride solution containing EDTA in advance.

The electrochemical characterizations of Al-doped spinel were determined in a screw cell. The method of assembling the cell was as follows: the cathode was 25 mg of accurately weighed active material and 15 mg of conductive binder (10 mg of Teflonized acetylene black (TAB) and 5 mg graphite). It was pressed on a 250 mm^2 stainless steel mesh as a current collector at 300 kg/cm^2 and dried at 200°C for 5 h in an oven. This cell consisted of a cathode and a lithium metal anode (Cyprus Foote Mineral Co.) separated by a porous polypropylene film as a separator (Celgard 3401). The electrolyte used was a 1:2 mixture of ethylene carbonate (EC) and dimethyl carbonate (DMC) containing 1 M $LiPF_6$ (Ube Chemical, Japan). All assembling of the cell was carried out in an argon-filled dry box. The charge and discharge cycling was galvanostatcically performed at a current density of 0.4 mA/cm^2 with a cut-off voltage of 3.0–4.3 V (versus Li/Li^+).

3. Results and discussion

These precursors were made using four types of Al-doped materials and two Mn-based materials to investigate the effect of substitution. Each starting material was calcined under various conditions as shown in Table 1. In order to obtain homogeneous samples, each sample was ground by ball milling thoroughly after precalcination. The crystal structure was indexed to a cubic system with a lattice parameter of $a = 8.23$–4 Å range and showed a high initial discharge capacity of over 130 mAh/g similar to that of pure spinel $LiMn_2O_4$.

Fig. 1 shows the thermal behavior of Al-doped precursors by simultaneous thermogravimetric analysis (TGA) and differential thermal analysis (DTA). The (a) mixture in this figure shows a discrete weight loss in TGA and one sharp exothermic peak in DTA at 660°C. The first endothermic peak of DTA at the temperature of 30–80°C is related to the removal of water. The second DTA peak shows that γ-MnOOH is transformed into β-MnO_2 at 260°C, which will improve the contact area between the lithium salt and the Mn salt. The third peak of DTA represents the formation of disordered Al-doped spinel at 410°C, which can increase the specific surface area of the resulting material. The last exothermic peak shows the decomposition of $Al(OH)_3$.

Table 1
Synthetic conditions and properties of $LiAl_xMn_{2-x}O_4$ powders

Sample	x in $LiAl_xMn_{2-x}O_4$	Starting materials	Precalcination temperature (°C)	Calcination temperature (°C)	Atmosphere	Lattice parameter (Å)	Intensity ratio of $I(3\,1\,1)/I(4\,0\,0)$	Initial discharge capacity(mAh/g)
1	0.03	$Mn_3O_4 + Al(NO_3)_3$	450	800	O_2	8.2318	0.9671	134
2	0.03	$Mn_3O_4 + Al(OH)_3$	300	800	O_2	8.2324	0.9885	132
3	0.03	$Mn_3O_4 + AlF$	450	700	Air	8.2265	0.9676	136
4	0.03	$Mn_3O_4 + Al_2O_3$	300	800	O_2	8.2356	0.9697	133
5	0.09	γ-MnOOH + $Al(NO_3)_3$	300	800	Air	8.2230	1.0871	126
6	0.09	γ-MnOOH + $Al(OH)_3$	300	800	Air	8.2306	1.1037	128
7	0.09	γ-MnOOH + AlF	450	800	Air	8.2359	1.1052	124
8	0.03	γ-MnOOH + Al_2O_3	300	800	Air	8.2288	1.0940	129

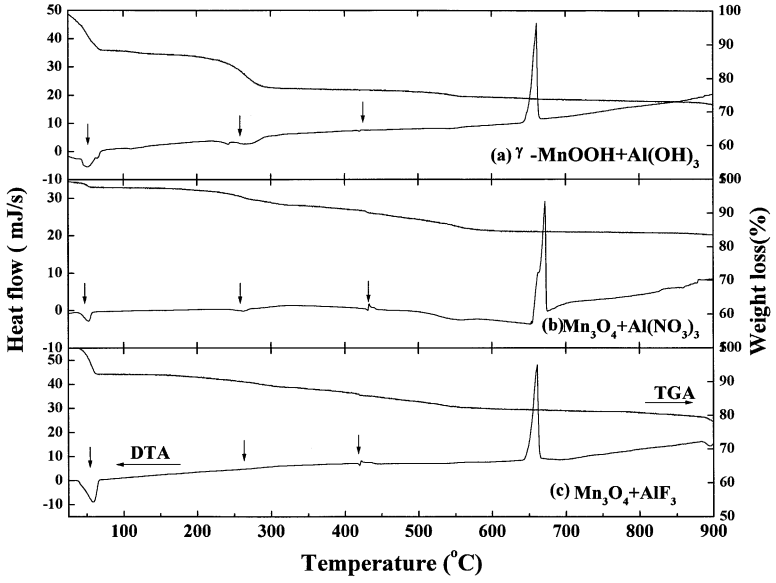

Fig. 1. Themogravimetric and differential thermal analyses for precursors, which were various Al salts mixed with Mn-based materials. All mixtures included Li compound. These mixtures were dried in a vacuum dryer at 100°C prior to thermal analysis and the heating rate was 5°C/min under N_2 atmosphere.

It exactly coincides with the Al melting point; the temperature is 660°C for all precursors. The (b) and (c) mixtures show very similar thermal behavior compared with the (a) mixture. Therefore, these mixtures were precalcined at 300 or 450°C for 10 h, respectively, which promotes the combination with other constituents. All precalcination temperatures for other mixtures in this research were determined in the same way.

Fig. 2 shows the XRD patterns of a series of powders with different x in $LiAl_xMn_{2-x}O_4$ materials at 800°C for 20 h in air atmosphere. This shows that we obtained pure Al-doped spinel without any impurity compared with that of the parent $LiMn_2O_4$ in this research. Although, the intensity ratio of (3 1 1)/(4 0 0) peaks increased slightly and the split in the (4 4 0) peak diminished according to the Al content, it is confirmed that this compound is coincident with a cubic unit cell with a space group $Fd\bar{3}m$. It is also well-known that the position and full width at half maximum (FWHM) of the (4 0 0) peak can an important factor indicating the degree of crystallinity in $LiMn_2O_4$ spinel powder. They [17] have announced that the mean lithium content of the spinel can be synthesized when the (4 0 0) peak is located at $2\theta = 43.95°$ and showed 0.1 value in FWHM. We found good agreement between our data and these results through silicon reference correction.

The first charge–discharge behavior of $LiAl_xMn_{2-x}O_4$ at various x contents (0.03–0.12) is plotted in Fig. 3. This sample was synthesized from LiOH, Mn_3O_4 and $Al(NO_3)_3$

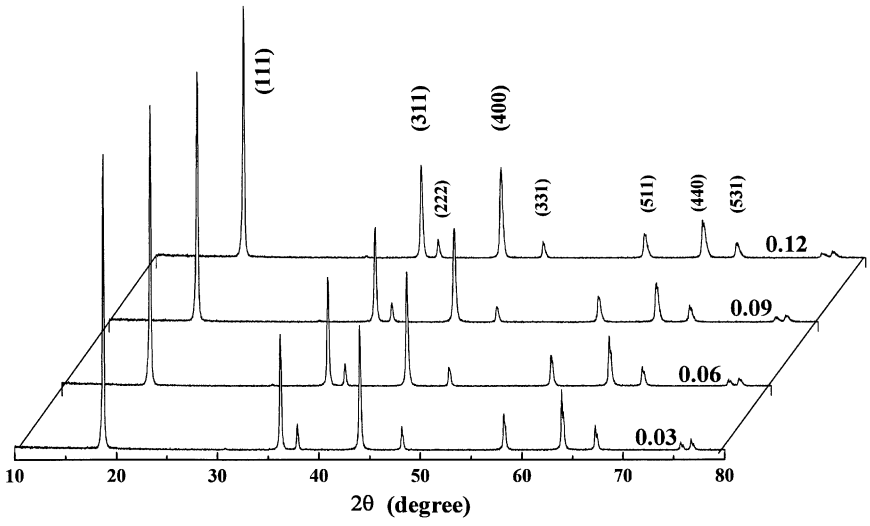

Fig. 2. X-ray diffraction patterns of $LiAl_xMn_{2-x}O_4$ powders calcined with various Al contents, the precursors were calcined at 800°C in air.

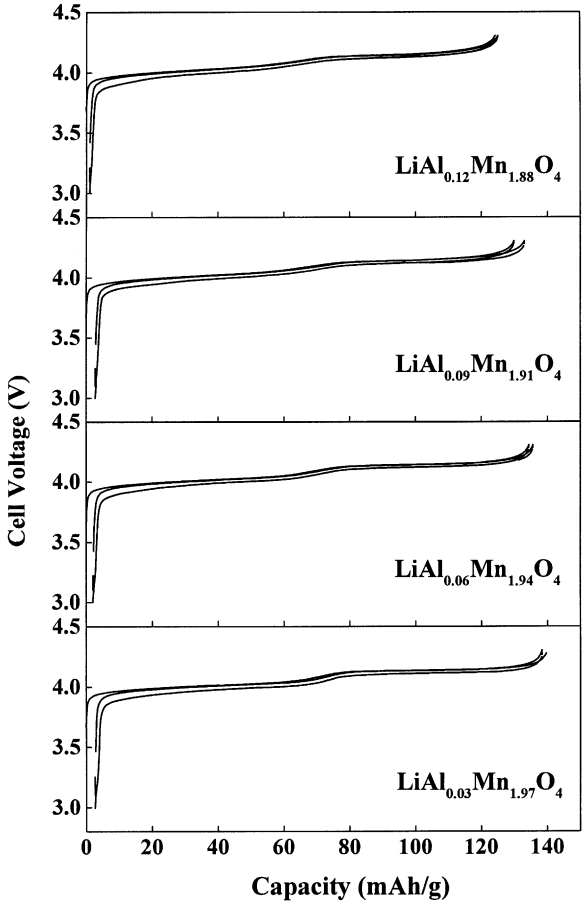

Fig. 3. Charge–discharge curves for Li/1 M $LiPF_6$-EC/DMC/$LiAl_xMn_{2-x}O_4$ cells using $LiM_xMn_{2-x}O_4$ calcined at 800°C in oxygen. The starting materials were LiOH, Mn_3O_4 and $Al(NO_3)_3$, cycling was carried out galvanostatically at a constant charge–discharge current density of 0.4 mA/cm^2 between 3.0 and 4.3 V.

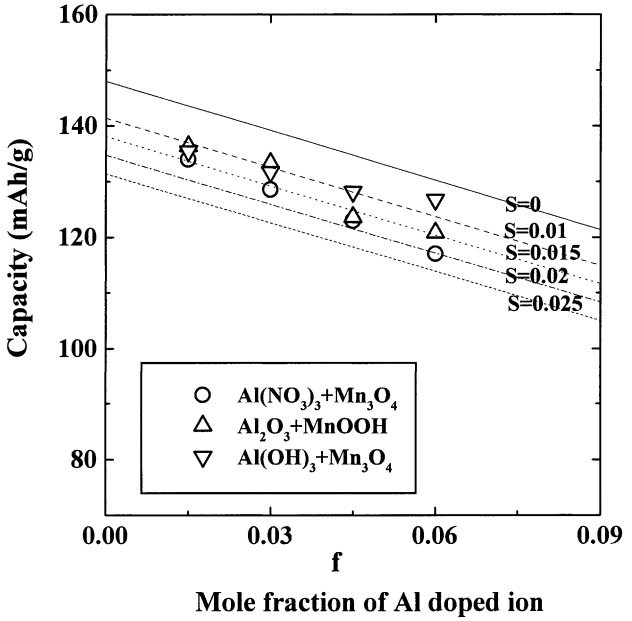

Fig. 4. Dependence of theoretical capacity and Al contents of $LiAl_xMn_{2-x}O_4$ powders on optimum calcined conditions. All starting materials included Li compound, s = vacancy content, $f = r/(p+q+r)$ of $(Li_x\square_{1-x})_{8a}(Mn(III)_pMn(IV)_qM(Z)_r\square_s)_{16d}O_4$.

starting materials and tested in 1 M $LiPF_6$-EC/DMC (1:2 by volume) solution at a constant charge–discharge current of 0.4 mA/cm^2. In proportion to the increase in the Al-doped content in this figure, two distinct plateaus regions at 4.0–4.15 V disappeared step-by-step very slowly. This corresponds to a lithium ion extraction/insertion from/into the tetrahedral (8a) sites. This phenomenon means that the Al ion was substituted exactly at the octahedral (16d) sites in cubic spinel and formed a solid solution with the spinel powder. The observed first discharge capacities of each sample are 133.5, 128.7, 125.8 and 121.9 mAh/g according to the Al content, respectively. If the Al ion could not be substituted at the 16d site perfectly, the movement of lithium in the cubic spinel might be hindered and this would be a reason for capacity fading on cycling.

Some groups [14,18,19] announced various methods to improve capacity retention in $LiMn_2O_4$, such as lithium-excess spinel ($Li_{1+x}Mn_2O_4$) or a metal-doped spinel such as $LiM_xMn_{2-x}O_4$ (M = Co, Ni, Mg, etc.). However, there was no remarkable merit, because it should sacrifice high initial discharge capacity to obtain good cycleability. Moreover, they could not ensure good cycleability after long-term cycling. In this research, although there is also a slight capacity decrease according to the increase in Al content, it is very small and the initial discharge capacity is the highest value for any results with Al-doped spinels in previous reports.

In our previous paper [20], we had proposed a good method to determine the theoretical capacity of metal ion-doped $LiMn_2O_4$ material. By using this method, it is possible to check easily oxidation number and vacancy content of different doped metal ions in spinel. Fig. 4 shows the dependence of the theoretical first charge capacity and the measured capacity for the Al-doped compound using various materials at each contents. Even if there is a slight difference in the first charge capacity in each sample, the observed capacities of all samples show a similar to theoretical capacity in tendency. All materials lie on the line of trivalent metal ion ($z = 3$) doped spinel and locate between $s = 0.01$ and 0.02 (s = vacancy content in 16d site). However, Al_2O_3+γ-MnOOH mixture shows a different behavior compare to other mixtures. Because the Al_2O_3 precursor is aqueous solution, it is a different phase compared with those of other Al starting materials, not a solid-solid reaction but a solid-liquid reaction, it may not be possible to retain a homogeneous state through the synthetic process in spite of impeccable ball milling because Al_2O_3 used is a very small amount. Although, there was a slight difference in the capacity between Al_2O_3 + γ-MnOOH mixture and other powders at $f = 0.06$, the results agree well with ideal behavior and show good cycle performance [20].

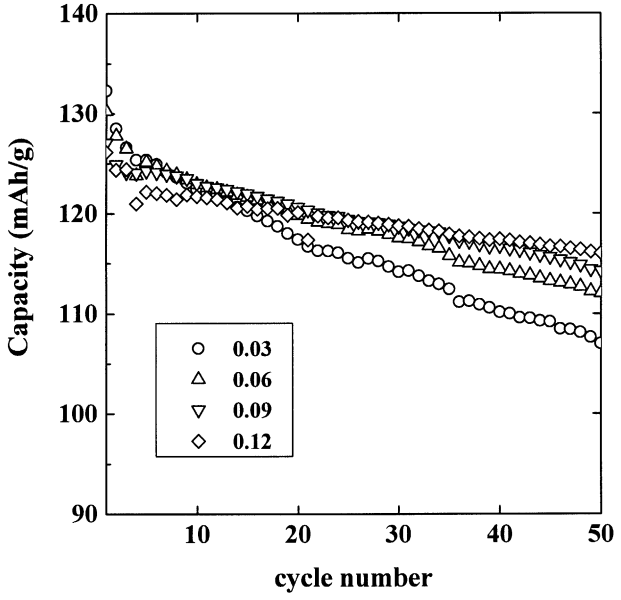

Fig. 5. The plot of specific discharge capacity vs. number of cycles for the Li/1 M $LiPF_6$-EC/DMC/$LiAl_xMn_{2-x}O_4$ cells with various Al contents. The starting materials were LiOH, Mn_3O_4 and $Al(OH)_3$, which were calcined at 800°C in oxygen atmosphere. Cycling was carried out galvanostatically at a constant charge–discharge current density of 0.4 mA/cm^2 between 3.0 and 4.3 V.

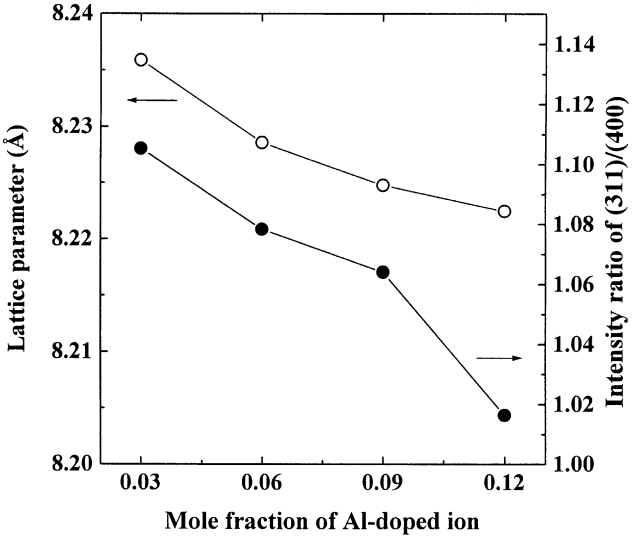

Fig. 6. Dependence of the lattice parameters and the intensity ratio of (3 1 1)/(4 0 0) peaks for the $LiAl_xMn_{2-x}O_4$ powders on the Al content. The starting materials were LiOH, γ-MnOOH and AlF_3, which were calcined at 800°C in air.

The relationship between the specific capacity and the cycle number of $LiAl_xMn_{2-x}O_4$ cells with various Al contents is plotted in Fig. 5. This powder was synthesized from a mixture of LiOH, Mn_3O_4 and $Al(OH)_3$ as the starting materials. Results show very good relation between initial capacity and cycleability which is affected by the Al doping amounts. As expected, the $LiAl_{0.03}Mn_{1.97}O_4$ shows the highest initial discharge capacity in all samples. However, the capacity faded faster than any other compositions. The $LiAl_{0.12}Mn_{1.88}O_4$ sample initially delivered 126 mAh/g and still delivered 116 mAh/g after 50 cycles. This cell shows good cycleability, which only decreased by 0.2 mAh/g per cycle on the average.

Fig. 6 shows the dependence of the lattice parameters and the intensity ratio of (3 1 1)/(4 0 0) peaks of various x contents in $LiAl_xMn_{2-x}O_4$ powder, which was synthesized using LiOH, γ-MnOOH and AlF_3 starting materials at 800°C for 20 h in an air flow. The more Al content increased, the less lattice parameter decreased from 8.2359 to 8.2255 Å. Because the ionic radius of Al^{3+} (0.57 Å) is smaller than that of Mn^{3+} (0.66 Å), if Mn^{3+} is replaced by Al^{3+} ion successfully, the lattice parameter will be decreased and will cause shrinkage of the structure. It shows that the Al content may be an important key parameter in extending cycle life of Al-doped materials. As far as the intensity ratio of (3 1 1)/(4 0 0) peaks is concerned, this will be referred to in the next figure.

In order to investigate the effect of the intensity ratio of (3 1 1)/(4 0 0) peaks in the Al-doped spinel, $LiAl_{0.09}Mn_{1.91}O_4$ was synthesized using LiOH, Mn_3O_4 and AlF_3

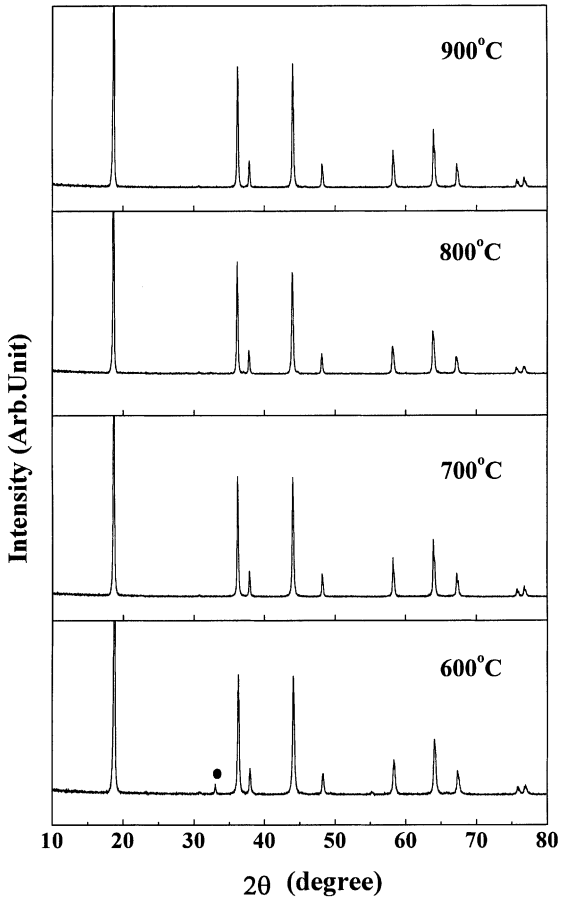

Fig. 7. X-ray diffraction patterns of $LiAl_{0.09}Mn_{1.91}O_4$ powders calcined at various temperatures for 20 h in air. The starting materials were LiOH, Mn_3O_4 and AlF_3.

starting materials at 600–900°C for 20 h in air. Fig. 7 shows the X-ray diffraction (XRD) patterns for the $LiAl_{0.09}Mn_{1.91}O_4$ compound at different temperatures. Pure XRD patterns appear in all temperature regions except for the 600°C sample. This indicates that the 600°C sample has poor crystallinity and impurities such as Mn_2O_3. It is more interesting that only the 800°C sample showed the characteristic indication, a (4 0 0) peak of small intensity, in the XRD pattern among the $LiAl_{0.09}Mn_{1.91}O_4$ compounds.

Although, a very pure XRD pattern of the Al-doped spinel at 800°C is shown in Fig. 7, the intensity ratio of (3 1 1)/(4 0 0) peaks was larger than that of the other powders and the lattice parameter increased up to 8.24 Å. This is a very large value compared with the other samples.

In order to determine the relationship of the above two factors, the Al-substituted content and the intensity ratio of (3 1 1)/(4 0 0) peaks, we did cycle testing using the $LiAl_{0.09}Mn_{1.91}O_4$ compound. Fig. 8 shows the discharge capacity of the Li/1 M $LiPF_6$-EC/DMC/$LiAl_{0.09}Mn_{1.91}O_4$ cells which calcined at various temperatures with the cycle number at a constant charge–discharge current of 0.4 mA/cm^2. As expected, the powder calcined at 800°C shows not only a low initial discharge capacity but also the poorest cycleability among the $LiAl_{0.09}Mn_{1.91}O_4$ samples using LiOH, Mn_3O_4 and AlF_3 starting materials. The 800°C sample initially delivers a discharge capacity of 112.5 mAh/g and the last capacity was 88.7 mAh/g after 25th cycles. From the series of experiments, it is evident that the intensity ratio of (3 1 1)/(4 0 0) peaks and the Al content are important key points in synthesizing Al-doped spinel with a high initial discharge capacity and good cycle retention at the same time. Therefore, these parameters can be used to forecast the battery performance of Al-doped spinel materials.

One more interesting thing, the intensity ratio of (3 1 1)/(4 0 0) peaks showed good cycle performance when it was 0.96∼1.1 as shown in Table 1 it represents different behavior depending on the Mn source although Al content is the same (see Sample 4, 8 in Table 1). Futhermore, in the case of the LiOH, Mn_3O_4 and Al_2O_3 complex, the ratio increased from 0.96 ($x = 0.03$) to 1.00 ($x = 0.12$) in $LiAl_xMn_{2-x}O_4$ powder. However, the LiOH, γ-MnOOH, and Al_2O_3 complex showed opposite behavior each other from 1.09 ($x = 0.03$) to 1.01 ($x = 0.12$). Although, there could be many factors that cause this phenomenon, it seems to strongly depend on the physico-chemical properties of the parent $LiMn_2O_4$ material such as the shape of the particle, the specific surface area and crystallinity. Also a slightly different (4 0 0) peak appeared in the XRD pattern of $LiAl_xMn_{2-x}O_4$ because each Mn-based material has unique characteristic. As a matter of fact, we could obtain a different XRD result, especially the intensity ratio of (3 1 1)/(4 0 0) peaks, for $LiMn_2O_4$ depending on the different Mn source. These facts lead to the assumption that the Mn source has an effect on its substituted materials. This will be reported more detail in the next paper.

The relationships between the Al content and the Mn ion amount are illustrated in Fig. 9. The reduction of the Mn^{3+} amount caused by Al substitution promoted the increase in the Mn^{4+} amount in the Al-doped spinel. This is a clue to explain the relation between the high average Mn valency and the small discharge capacity in $LiAl_xMn_{2-x}O_4$ cell. Additionally, when the spinel precursor was calcined at high temperature, it showed a smaller FWHM value and a lower average oxidation state of Mn than that calcined at low temperature [16]. The spinel powders calcined at high

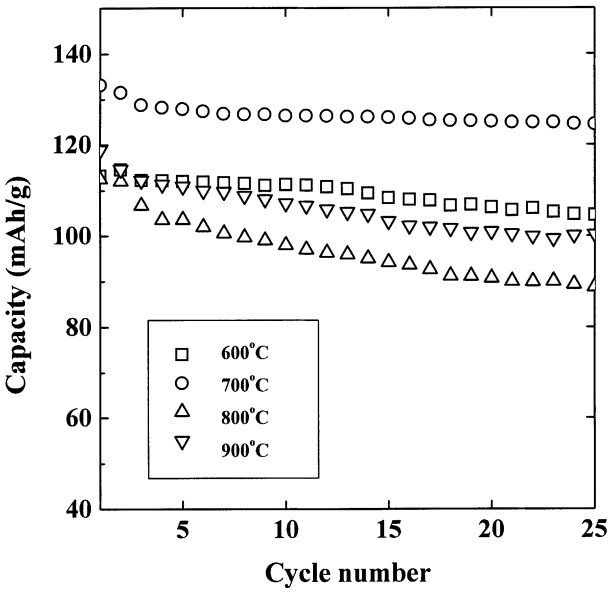

Fig. 8. The plot of specific discharge capacity vs. number of cycles for the Li/1 M $LiPF_6$-EC/DMC/$LiAl_{0.09}Mn_{1.91}O_4$ cells using LiOH, Mn_3O_4 and AlF_3 at various temperatures. Cycling was carried out galvanostatically at a constant charge–discharge current density of 0.4 mA/cm^2 between 3.0 and 4.3 V.

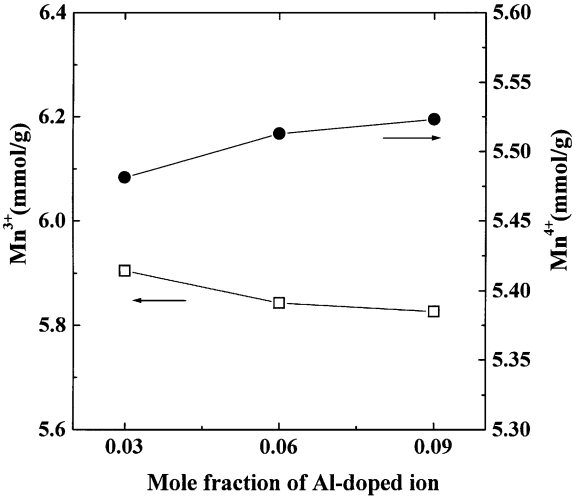

Fig. 9. Dependence of Mn ion amount and Al contents for the $LiAl_xMn_{2-x}O_4$ powder. The starting materials were LiOH, Mn_3O_4 and $Al(OH)_3$, which were calcined at 800°C in air.

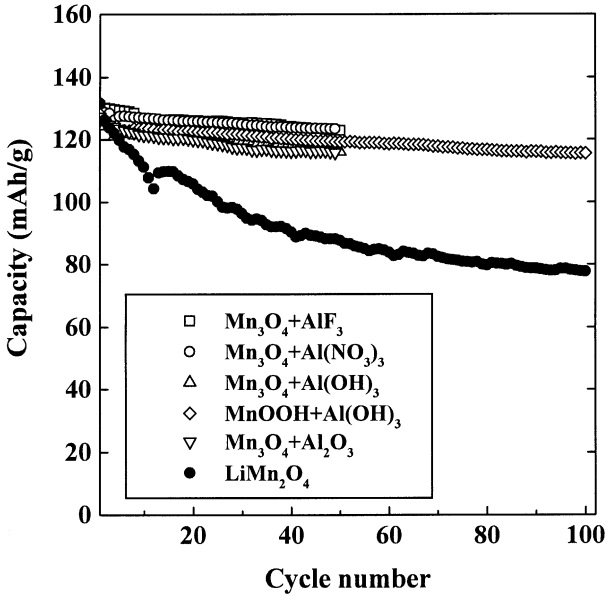

Fig. 10. Variation in specific discharge capacity with number of cycles for the Li/1 M $LiPF_6$-EC/DMC/$LiAl_xMn_{2-x}O_4$ cells using various Al starting materials. Cycling was carried out galvanostatically at a constant charge–discharge current density of 0.4 mA/cm^2 between 3.0 and 4.3 V.

temperature are thought to have higher crystallinity and high initial capacity. Although, it is possible to form a defect spinel ($Li_{1-x}Mn_{2-x}O_4$) and decrease the average Mn valency under 3.5 at high calcination temperature, it is reasonable that an increase in Mn^{4+} content in the spinel encourages good cycleability.

Fig. 10 shows the relation of specific discharge capacity with the cycle number of Al-doped spinels using various Al starting materials at a constant charge–discharge current density of 0.4 mA/cm^2. The test was done between 3.0 and 4.3 V at room temperature. The x value of $LiAl_xMn_{2-x}O_4$ is 0.09–0.12 in all samples. The cycle behavior of stoichiometric $LiMn_2O_4$ is also shown in this figure. The $LiMn_2O_4$ sample shows poor cycleability although it has a high initial discharge capacity on the first cycle. However, most Al-doped spinels in this research showed not only high initial discharge capacity above 125 mAh/g but also very good rechargeability. The capacity retention rate of LiOH, Mn_3O_4, and $Al(OH)_3$ mixture after 100 cycles was 90% of the initial capacity in all Al-doped compounds.

On the basis of these results, it is concluded that replacing the Mn^{3+} ion by Al^{3+} increased the average oxidation state of the Mn ion, and it help to retain an average Mn valency higher than 3.5 in $LiAl_xMn_{2-x}O_4$ powder. It also works to maintain a single phase through the charge–discharge process (see Fig. 3). Therefore, this can be a means of enhancing the cycleability of $LiMn_2O_4$ in electrochemical cycling.

It seems that an excellent method for the preparation of Al-doped spinel can be the melt-impregnation method, which was used in this research. We also expect that the cycle behavior of Al-doped spinel may show different characteristics in the high temperature region(>50°C). Therefore, it is necessary to establish the optimum synthesis conditions and environment in our future work.

4. Conclusions

The $LiAl_xMn_{2-x}O_4$ has been synthesized using various aluminum starting materials, such as $Al(NO_3)_3$, $Al(OH)_3$, AlF_3 and Al_2O_3 at 600–800°C for 20 h in air or oxygen atmosphere. Pure Al-doped spinel was obtained without any impurity in the XRD patterns. As the Al content increased, the lattice parameter, a, decreased because the ionic radius of Al^{3+} (0.57 Å) is smaller than that of Mn^{3+} (0.66 Å). The Al content and the intensity ratio of (3 1 1)/(4 0 0) peaks may be important parameters for synthesizing Al-doped spinel, which satisfies the requirements of high discharge capacity and good cycleability at the same time. The decrease in the Mn^{3+} ion by Al substitution increased the average Mn valency in the $LiAl_xMn_{2-x}O_4$ powder. This helps to maintain a single phase through the charge–discharge process. The electrochemical behavior of all samples was studied in Li/$LiPF_6$-EC/DMC (1:2 by volume)/$LiAl_xMn_{2-x}O_4$ cells. The initial and last discharge capacity of the LiOH, Mn_3O_4, and $Al(OH)_3$ complex were 128.7 and 115.5 mAh/g after 100 cycles when x was 0.09 in $LiAl_xMn_{2-x}O_4$. The Al-doped spinel was a means of enhancing the cycleability of stoichiometric $LiMn_2O_4$ during electrochemical cycling. The melt-impregnation method used in this research is a very excellent process for synthesizing Al-doped spinel with high initial discharge capacity as well as good cycleability at the same time.

References

[1] K. Mizushima, P.C. Jones, P.J. Wiseman, J.B. Goodenouh, Mater. Res. Bull. 15 (1980) 783.
[2] C. Plichata, M. Salomon, S. Slane, M. Uchiyoma, B. Chua, W.B. Ebner, H.W. Lin, J. Power Sources 21 (1987) 25.
[3] J.R. Dahn, U. Von Sacken, C.A. Michel, Solid State Ionics 44 (1990) 87.
[4] T. Ohzuku, J. Kato, K. Sawai, T. Hirai, J. Electrochem. Soc. 138 (1991) 2556.
[5] J.R. Dahn, E.W. Fuller, M. Obrovac, U. Von Sacken, Solid State Ionics 69 (1994) 265.
[6] Z. Zhang, D. Fouchard, J.R. Rea, J. Power Sources 70 (1998) 16.
[7] D. Guyomard, J.M. Tarascon, Solid State Ionics 69 (1994) 222.
[8] Y. Xia, H. Takeshige, H. Noguchi, M. Yoshio, J. Power Sources 56 (1995) 61.
[9] Y. Gao, J.R. Dahn, J. Electrochem. Soc. 143 (1996) 100.
[10] W. Liu, G.C. Farrington, F. Chaput, B. Dunn, J. Electrochem. Soc. 143 (1996) 879.
[11] D.H. Jang, Y.J. Shin, S.M. Oh, J. Electrochem. Soc. 143 (1996) 2204.
[12] D.H. Jang, Y.J. Shin, S.M. Oh, J. Electrochem. Soc. 144 (1997) 3342.

[13] Y. Xia, Y. zhou, M. Yoshio, J. Electrochem. Soc. 144 (1997) 2593.
[14] Q. Zhone, A. Bonakdarpour, M. Zhang, Y. Gao, J.R. Dahn, J. Electrochem. Soc. 144 (1997) 205.
[15] F. Le Cras, D. Bloch, M. Anne, P. Strobel, Solid State Ionics 89 (1996) 203.
[16] Y. Xia, M. Yoshio, J. Power Sources 57 (1995) 125.
[17] V. Manev, T. Faulkner J. Engel, in: Proceedings of the HBC98, The first Hawaii Battery Conference, 1998, p. 228.
[18] J. Gummow, A. Kock, M.M. Thackeray, Solid State Ionics 69 (1994) 59.
[19] M. Yoshio, H. Noguchi, T. Miyashita, H. Nakamura, A. Kozawa, J. Power Sources 54 (1995) 483.
[20] Y.M. Todorov, Y. Hdeshima, H. Noguchi, M. Yoshio, J. Power Sources 77 (1999) 198.